DE GRUYTER Energy Harvesting and Systems 2016; 3(1): 101–111

Lukas Stepien*, Aljoscha Roch, Sarah Schlaier, Ines Dani, Anton Kiriy, Frank Simon, Marian v. Lukowicz and Christoph Leyens

Investigation of the Thermoelectric Power Factor of KOH-Treated PEDOT:PSS Dispersions for Printing Applications

DOI 10.1515/ehs-2014-0060

Abstract: This work studies the modification of commercially available dispersions of intrinsically conductive polymer PEDOT:PSS with a strong base, KOH. It is concluded that addition of base derives a dedoping of the PEDOT chain and increase Seebeck coefficient from 15 μV/K to 90 μV/K. Supportive UV-Vis-NIR spectroscopy was used for tracking the doping level of the polymer. A surface morphology study of the dedoped PEDOT:PSS films was monitored by SEM. It was shown that if KOH is used in excess with respect to the acid component of PEDOT:PSS dispersions, it segregates at the surface forming crystallites. They, however could be easily removed by methanol rinsing without destroying the sample integrity. After material modification, a dispenser-printed polymer unileg-TEG with 61 unicouples was fabricated by printing. The TEG in form of 253 mm-long stripe shows a flexible behavior. At 90 K temperature difference a resulting power output of ~ 100 nW could be measured. We suggest that the low power output is due to a high internal generator resistance.

Keywords: flexible, intrinsically conducting polymer, PEDOT:PSS, power factor, printing, de-doping, thermoelectric generator, base, pH value

Introduction

Thermoelectric energy harvesting exhibits the unique ability to convert thermal energy directly into electrical energy. A thermoelectric generator (TEG) placed between a heat source and heat sink will cause a thermal gradient inside the TEG resulting in a current flow which can be directly used. The dimensionless figure of merit, $zT = \alpha^2\sigma T/\kappa$ summarizes the thermoelectric performance of a material by combining the Seebeck coefficient α, the electrical conductivity σ, the thermal conductivity k and the ambient temperature T.

The materials with reasonable thermoelectric properties are usually heavily doped semiconductors showing several disadvantages for potential applications like e.g. poor mechanical stability, high brittleness or the use of rare abundant elements. However, much effort was put in the development of intrinsically conductive polymers (ICP) within the last decade which can overcome these challenges due to their polymer nature (Park 1991). The advantages over other material classes are ease of processing (e.g. by state of the art printing technologies), availability (no use of rare elements) and mechanical flexibility (for flexible TEGs).

For thermoelectric applications, different conducting polymers such as, polyacetylene (Zuzok et al. 1991), polyanilines (Mateeva et al. 1998; Yan, Sada, and Toschima 2002) or polythiophenes (Osterholm et al. 1987; Masubuchi et al. 1993) were investigated.

Particularly, poly(3,4-ethylenedioxythiophene):poly (styrenesulfonate) (PEDOT:PSS) (Kim et al. 2013) and poly(3,4-ethylenedioxythiophene):iron tosylate (PEDOT: tos) (Bubnova et al. 2011) are among most promising thermoelectric materials which show relatively high zT values of 0.42 and ~1, respectively.

PEDOT:PSS is perhaps the most studied and widely used conducting polymer, yet it is commercially available at a large scale. However PEDOT itself, as well as other pi-conjugated polymers in their pristine, undoped form have low electrical conductivity. Conductive, yet water-dispersible form of PEDOT is formed upon oxidative

---

***Corresponding author: Lukas Stepien,** Fraunhofer Institut für Werkstoff- und Strahltechnik IWS, 01277 Dresden, Germany, E-mail: lukas.stepien@iws.fraunhofer.de
Aljoscha Roch: E-mail: aljoscha.roch@iws.fraunhofer.de, **Sarah Schlaier:** E-mail: sarah.schlaier@iws.fraunhofer.de, **Ines Dani:** E-mail: ines.dani@iws.fraunhofer.de, Fraunhofer Institut für Werkstoff- und Strahltechnik IWS, 01277 Dresden, Germany
Anton Kiriy: E-mail: kiriy@ipfdd.de, **Frank Simon:** E-mail: frsimon@ipfdd.de, Leibniz-Institut für Polymerforschung Dresden e.V., 01069 Dresden, Germany
Marian v. Lukowicz, Technische Universität Dresden, Institut für Luft- und Raumfahrttechnik, 01307 Dresden, Germany, E-mail: marian.von_lukowicz@tu-dresden.de
Christoph Leyens, Fraunhofer Institut für Werkstoff- und Strahltechnik IWS, 01277 Dresden, Germany; Technische Universität Dresden, Maschinenwesen, 01069 Dresden, Germany, E-mail: christoph.leyens@iws.fraunhofer.de

polymerization of EDOT conducted in the presence of polystyrene sulfonic acid (PSA). In this polymerization, persulfates are typically used as both oxidative polymerization agents and the agent, partially oxidizing pi-conjugated backbone of thus-formed PEDOT chains. The process of oxidation of neutral chains into charge carriers – positively charged polarons and bipolarons – is called a primary doping, according to MacDiarmid concept (MacDiarmid and Epstein 1994). At the same time, PSA in its ionized form acts as negatively charged counter ions. Furthermore, because PSA is typically taken in an excess, ionized sulfonic acid groups provide a neat negative charge to colloidal PEDOT:PSS particles and ensures their colloidal stability in water.

In addition, it was demonstrated that excess of PSA as well as other strong acids significantly enhances conductivity of oxidatively-doped PEDOT (Ouyang 2013). This process is more well-known in the case of easily protonable polyanilines having well-pronounced basic nature; however, EDOT oligomers were also shown to undergo protonation in the presence of sulfuric acid, organosulfuric acids, trifluoroacetic acid, etc. (Elschner et al. 2010). Although exact mechanism of the conductivity enhancement was not clarified, a direct protonation of not fully doped PEDOT chains in the alfa-position by thiophenic sulfur leading to species structurally similar to the structures formed upon oxidative doping (bipolarons), is a most probable explanation of this phenomenon. Along this line, it was shown that treatment of heavily doped PEDOT:PSS dispersions with strong bases (NaOH) leads to a significant decrease in conductivity of PEDOT:PSS accompanied with a decrease of intensity of bipolaron absorption, i.e., transformations usually observed upon more “classical” dedoping induced by addition of reducing agents (de Kok et al. 2004; Weijtens 2005). Because it is clear that NaOH and similar bases cannot act as reducing agents, other, non-redox dedoping mechanisms should be operative in this case. Although authors of the Kok et al. work explained base-induced dedoping to complex structural rearrangements occurring inside PEDOT:PSS particles upon pH increase, we instead suggest that a simple deprotonation of initially heavily protonated PEDOT chains is a more probable reason of the decreased conductivity.

It was previously demonstrated that the *zT* of thermoelectric materials strongly depends on concentration of charge carriers (holes or electrons) (Snyder and Toberer 2008) which, in turn, is controlled by the doping degree. The control of the doping level in PEDOT was performed by several groups with electrochemical treatment (Ahonen, Lukkari, and Kankare 2000; Lock et al. 2007; Bubnova et al. 2011; Park et al. 2013) or change of solvents (Kim et al. 2002, 2005, 2013; Ouyang et al. 2004; Meen et al. 2013). Recently, Massonnet et al. (2014) presented the wet chemical reduction of PEDOT:PSS by casting reducing agents onto prepared PEDOT films in order to improve the Seebeck coefficient. However, chemical treatments after film preparation are not desirable as they complicate the technological process. Printing of thermoelectric polymers is perhaps the most attractive way for TEG fabrication, as it offers the possibility for an efficient and industrial compliant TEG production (Chen et al. 2011; Dani et al. 2013). For a TEG based on an n- and p- type organic-metal complex a power output of 1 μW/cm^2 at temperature difference of 25K could be shown. The zT values of the used material were in the range of 0.1–0.2 (Sun et al. 2012). The power outputs of PEDOT-based TEGs are in the range of 0.27 μW/cm^2 with an applied temperature gradient of 30K. This result was gained by using a strongly doped and afterwards reduced (dedoped) PEDOT polymer (Bubnova et al. 2011). However, for printed TEGs post-treatments associated with electrochemical modifications are not feasible. On the other hand, wet chemical modifications before film formation seems more meaningful approach for the fabrication of printed TEG.

Interestingly, although the use of reducing agents (i.e., primary doping process) for tuning of PEDOT:PSS thermopower was extensively reported (Kim et al. 2013), influence of pH value (i.e., secondary doping process) on its Seebeck coefficient was not addressed. Here, we report on the modification of the thermoelectric power factor, $PF = \alpha^2 \cdot \sigma$ of PEDOT:PSS dispersions by wet chemical treatment with a strong base, KOH. The aim is to produce a modified thermoelectric ink that can be directly applied by common printing techniques without the necessity for further reduction steps. This offers the opportunity for ink preparation and TEG printing in an economical way. We show that the reduced PEDOT:PSS ink can be used for the printing of flexible TEG strips.

Methods

Chemicals

PEDOT:PSS (Clevios^{TM} PH 1000 and Clevios^{TM} SV3) was supplied by Heraeus Clevios GmbH. Isopropyl alcohol (IPA, purity > 99.5 %) was purchased from Carl Roth. The reducing agent Potassium hydroxide (KOH, Reagent A.C.S.) was purchased from Merck Millipore.

Silver paste (5025 Polymer Silver Conductor) for printing conductive lines was purchased from DuPont. Polyimide foil (thickness 75 µm) supplied by RS Components was used as substrate for the printed TEG.

Equipment

The electrical conductivity was measured by 4-point probe (Euris GmbH) at room temperature. The measurement of the Seebeck coefficient was done by a home build setup at room temperature. The Seebeck measurement setup is composed of two spring loaded thermocouples for the measurement of the thermovoltage and temperature difference. The distance between the thermocouples was set to 25 mm. The mounted samples where clamped directly with a heater (PT100 element) and a heat sink (Peltier element with copper block). The applied temperature difference was 10 K. Comparing measurements with commercial available setups (SRX from Fraunhofer IPM and ZEM-3 from Ulvac) showed good accordance for measurements at room temperature.

Printing of PEDOT:PSS SV3 and silver paste was performed by a dispenser printer (Dispense Mate, Asymtek). After cutting, the polyimide substrates were cleaned with IPA in an ultrasonic bath (Bandelin) for 5 min. Subsequently the substrates were immersed with IPA and dried under compressed air flow. The silver paste, acting as contacts and interconnections between the PEDOT:PSS elements, was printed first. A drying step at 100 °C for 10 min was performed in order to remove solvents followed by a curing step at 150 °C for 10 min. Afterwards, PEDOT:PSS was printed. Up to eight layers of PEDOT:PSS were printed in order to increase the cross section of the polymer legs. After printing each layer of PEDOT:PSS, a drying step for 30 min with 100 °C was done. A schematic view of the unileg-TEG is shown in Figure 1.

The dried TEG strip was rolled up on a cylindrical adapter. The characterization of the TEG strips where performed in a self-made TEG measurement setup (at Technical University of Dresden) in air. The output voltages where measured with loads between 6 and 15 kΩ according to the internal resistance of the TEG at temperature differences between 10 and 90 K.

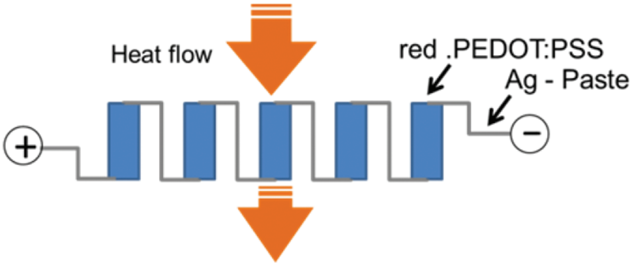

Figure 1: Schematic representation of a printed unileg-TEG.

The optical characterization of spin coated polymer films were performed with a UV-Vis-NIR spectrometer Cary 5000 (Agilent Technologies). PEDOT:PSS thin films were prepared with Clevios^{TM} SV3 on glass slides (Carl Roth) of 26 $\times$ 26 mm^2. The glass slides were cleaned in an ultrasonic bath containing acetone and IPA for 10 min each. Subsequently glass substrates were rinsed with IPA and dried under Nitrogen flow. After spin-coating, PEDOT:PSS films were dried at 80°C for 5 min on a hot plate. The film thicknesses of the prepared thin films were measured with a confocal microscope (Leica DCM 3D). The thicknesses were in the range of 140 and 280 nm depending on the viscosity due to the concentration of the base.

All XPS studies were carried out on spin-coated PEDOT:PSS PH1000 samples by means of an Axis Ultra photoelectron spectrometer (Kratos Analytical, Manchester, UK). The spectrometer was equipped with a monochromatic Al Kα ($h \cdot \nu = 1486.6$ eV) X-ray source of 300 W at 15 kV. The kinetic energy of photoelectrons was determined with a hemispheric analyzer set to pass energy of 160 eV for wide-scan spectra and 20 eV for high-resolution spectra. During all measurements, electrostatic charging of the sample was avoided by means of a low-energy electron source working in combination with a magnetic immersion lens. Later, all recorded peaks were shifted by the same value that was necessary to set the C 1s peak to 284.90 eV, which was assumed as reference value for the π-conjugated carbon-carbon and carbon-sulfur bonds (Oeter, Ziegler, and Göpel 1993). Quantitative elemental compositions were determined from peak areas using experimentally determined sensitivity factors and the spectrometer transmission function. Spectrum background was subtracted according to Shirley. The high-resolution spectra were deconvoluted by means of the Kratos spectra deconvolution software. Free parameters of component peaks were their binding energy (BE), height, full width at half maximum and the Gaussian–Lorentzian ratio.

The measurement of the Seebeck coefficient was performed on PEDOT:PSS thick films prepared by drop casting on 26 $\times$ 15 mm^2 glass substrates. The conditions were the same as for the thin film preparation. The resulting film thickness was in the range of 5–40 µm.

Preparation of modified PEDOT:PSS

PEDOT:PSS Clevios^{TM} SV3 printing paste and Clevios^{TM} PH1000 suspension were mixed with a magnetic stirrer for 1 h with different concentrations up to 240 mM (mmol/l) of KOH. A 1 molar solution of KOH was prepared and added drop wise under permanent stirring. To prevent ageing, all samples were processed and characterized within 1 h after preparation.

Results and discussion

Effect of KOH on PEDOT:PSS PH1000

KOH is known as a strong base which can be easily dissolved in water and it was used for changing the pH value of the PEDOT:PSS dispersions (see Figure 2) in the range from 1.8 to 13.

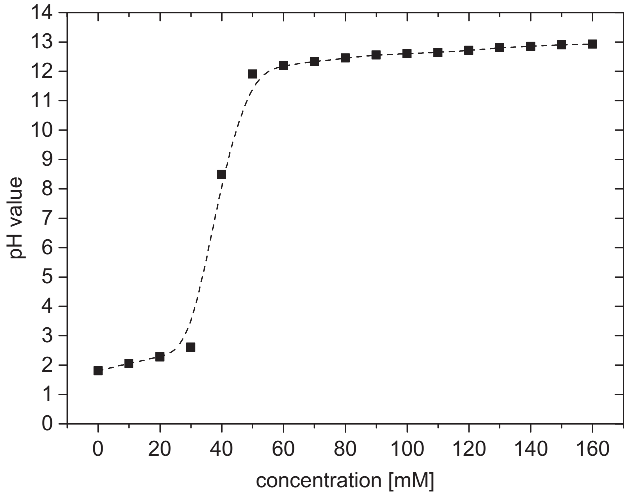

Figure 2: pH of the PH1000 dispersion on concentration of added KOH.

After adding KOH the dispersion was stirred until a constant pH value was set. A relatively prolonged stirring was necessary for reaching an equilibrium because of a limited accessibility of internal PEDOT:PSS fraction caused by a strongly aggregated nature of PEDOT:PSS. Particularly, constant pH values were achieved in strongly acidic and alkaline conditions after 15–20 min while near the equivalence point where the dispersion is neutral (pH value of 7) constant pH value was achieved after 1 h. The equivalence point was found for a KOH concentration of around 35 mM. The influence of the KOH concentration on the Seebeck coefficient will be discussed later.

Figure 3, left shows the flow curves of PEDOT:PSS dispersions with different KOH concentrations. In general, the PEDOT:PSS exhibits a shear thinning behavior dependent on the KOH concentration as a result of alignment of solvated polymer chains along to the shear direction. In the case of PEDOT:PSS, the solvated PSS chains are more entangled at lower shear stress leading to a higher viscosity. By applying shear stress, viscosity decrease caused by less entangled PSS chains.

By adding KOH, the shear viscosity (at a shear rate of $10\ s^{-1}$) is increased nearly by one order of magnitude from 0.05 Pa s to 0.42 Pa s (shown in Figure 3, right). The influence of KOH addition on the shear viscosity is more pronounced at lower shear rates. At the KOH concentration of 140 mM (shear rate of $0.1\ s^{-1}$), the shear viscosity is increased by more than three orders of magnitude when compared to the pristine PEDOT:PSS. It was observed that for high KOH concentrations the PEDOT:PSS dispersions become gel-like. At this point, it should be emphasized that this kind of modification may not be applicable for all kind of printing techniques. However,

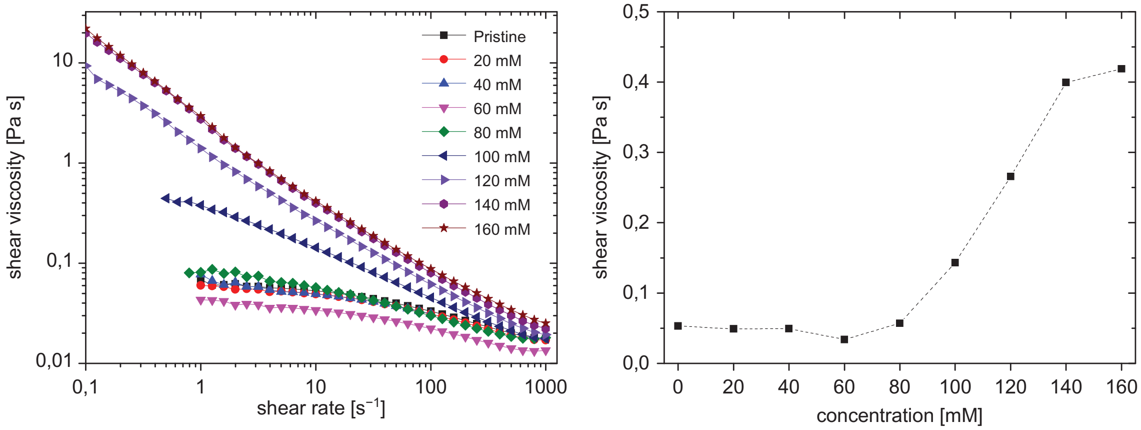

Figure 3: Flow curves of PEDOT:PSS PH1000 with different KOH concentrations (left) and shear viscosity of PEDOT:PSS PH1000 with different KOH concentrations at constant shear rate of $10\ s^{-1}$ (right).

inks always undergo some amount of shear stress during the processing/printing. Typically, shear rates during printing (e.g. ink jet, screen printing, etc.) are between 10^3 and 10^4 s^{-1}. The differences in the shear viscosity become smaller when going to higher shear rates.

The increased viscosity of the PEDOT:PSS dispersion leads to higher film thicknesses after spin coating. It was observed that with the introduction of KOH, the PEDOT:PSS dispersion tends to become gel-like above concentrations of 80 mM. Above this concentration no flowing is observed when turning the vial upside-down. Despite this, no phase separation, change in rheological behavior, formation of agglomerates or change in thermoelectrical properties could be observed within 3 months. Therefore it can be stated that the inks/paste printing performance as well as TE performance is stable in the observed time frame. However, with increasing KOH concentration, the number of gel-like agglomerates remaining on the thin films increase. It could be observed that these agglomerates are more likely formed during or after spin coating, since the use of a syringe filter showed first no agglomerates after casting the dispersion on the substrate but agglomerates after drying. To note, these agglomerates are in the sub-millimeter range and show a dark blue color. The increased viscosity of the PEDOT:PSS dispersions as well as aggregation (gelation) observed upon increase of amount of added KOH is clearly associated with the change in the pH value and can be explained as follows. In acidic dispersions, association of PSS and PEDOT involves two mechanisms. The first association mechanism is electrostatic interactions between positively charged doped (oxidized) PEDOT chains and negatively charged ionized PSS chains. The second mechanism assumes the protonation of undoped portion of PEDOT chains by strongly acidic PSA groups followed by attraction of positively charged protonated PEDOT chains to ionized PSS. Increase of pH value up to the alkaline conditions eliminates the second mechanism which results in a detachment of a fraction of PSS. It is also possible that addition of KOH weakens binding of the PSS fraction associated by electrostatic mechanism because in this case added hydroxyl anions can (partly) replace the PSS anions. Whatever the mechanism, the increase of pH leads to detachment of some fraction of hydrophilic PSS chains which, in turn leads to further aggregation of intrinsically hydrophobic PEDOT.

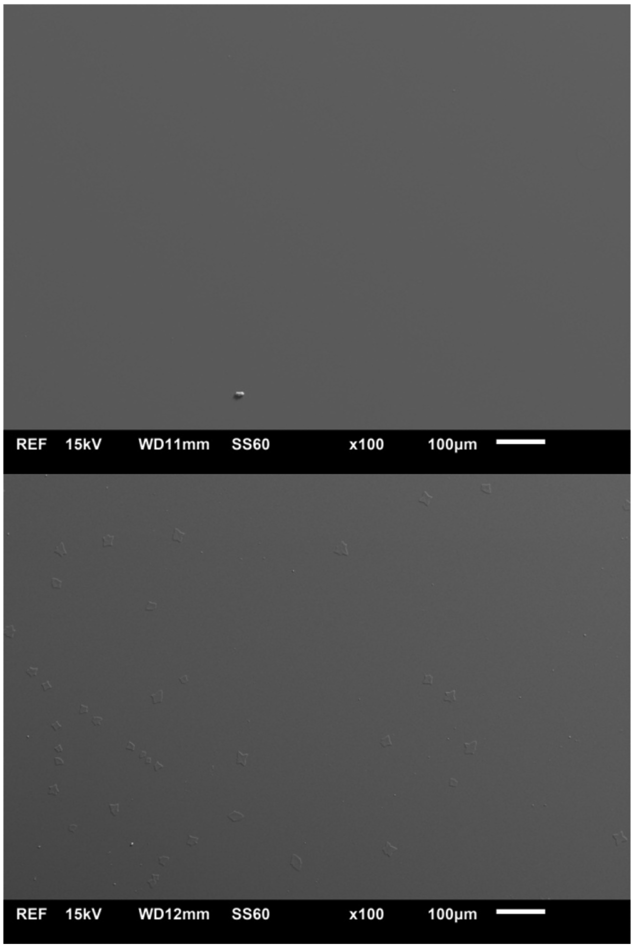

Figure 4: SEM image of spin-coated pristine (left) and KOH modified (right) PEDOT:PSS thin films.

It should be noted that the formation of small KOH and/or K_2CO_3 crystals on the surface was observed for spin coated films prepared from dispersions with added KOH for concentrations higher than 70 mM. Thus is undesirable phenomenon because KOH crystals represent an electrically isolating material (see Figure 4). However, an excess of KOH on the surface could be easily removed by methanol rinsing without changing of the film integrity. It should be also noted that water is less suitable solvent for removing of excess of KOH as it destroys PEDOT:PSS films. We performed XPS measurements to shed more light onto transformations occurring upon KOH-treatment.

XPS studies of PEDOT:PSS-KOH

XPS was employed to investigate chemical changes after KOH addition and film formation. Figure 5 shows high-resolution XPS spectra recorded from a pristine PEDOT:PSS sample and a sample, which was modified with KOH. Apart from the K $2p_{3/2}$ and K $2p_{1/2}$ peaks appearing after the KOH treatment, the C 1s spectra of both samples are nearly identical. The assignments of the three component peaks A, B, and C to the chemical structure of the PEDOT

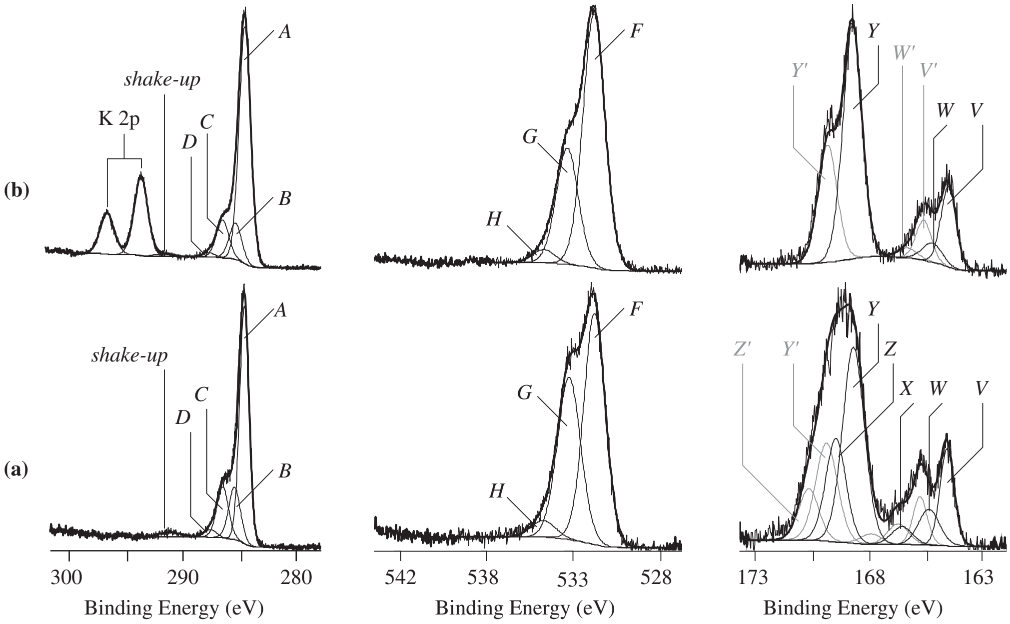

Figure 5: High-resolution C 1s (left column), O 1s (middle column), and S 2p (right column) XPS spectra recorded from pristine (a) and KOH modified (b) PEDOT:PSS PH1000 samples.

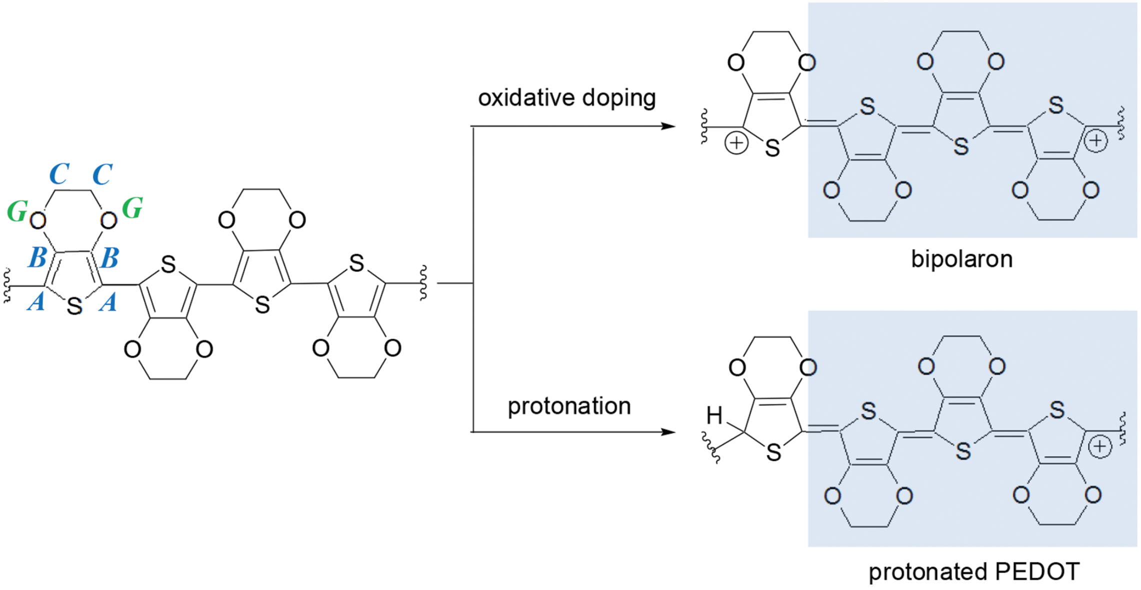

Figure 6: Oxidative doping and protonation of neutral PEDOT lead to very similar structures (marked by blue boxes). The assignments in italics (left structure) illustrate the different binding states of carbon and oxygen, which was detected in the high-resolution XPS spectra.

molecule is shown in Figure 6 (left) (Beamson and Briggs 1992; Jönnson et al. 2003). The origin of the additional small component peaks *D* is not very clear. They could arise from carbonyl carbons of keto or quinone-like groups (C = O) formed as byproducts during synthesis. After the KOH treatment, the intensity of component peak *A* seemed to be slightly increased. Obviously, small amounts of hydrocarbons were adsorbed on the sample surface. For samples, which were treated in wet-chemical processes the analysis of such surface contaminations is very common in surface spectroscopy.

Shake-up peaks resulting from $\pi \rightarrow \pi^*$ electron transitions indicate the presence of conjugated π-electron systems in the PEDOT molecules. The O 1s spectra of both samples are composed of three component peaks *F*, *G*, and *H* (Figure 5, middle column). While component peak

G shows the oxygen atoms of the PEDOT molecules (Figure 6), component peak *F* appeared from the almost completely dissociated sulfonic acid groups ($R\text{–}S\underline{O}_3^-$) (Beamson and Briggs 1992). The binding energy values found for component peaks *H* at 534 eV indicates the presence of water (Russat 1988) which is entrapped as solvating agent in the polymer films. Due to the *spin-orbit-interaction* all S 2p spectra are composed of the S $2p_{3/2}$ and S $2p_{1/2}$ peaks. That means, each binding state of sulfur contributes with two component peaks (assigned by e.g. *X* for the S $2p_{3/2}$ peak and *X′* for the S $2p_{1/2}$ peak; in Figure 5 not all S $2p_{1/2}$ component peaks were assigned) having a binding energy difference of 1.18 eV and an intensity ration of [S $2p_{3/2}$]:[S $2p_{1/2}$] = 2:1 to the high-resolution S 2p spectrum (Moulder et al. 1992). As can be seen in Figure 5 (right column) the S 2p spectrum recorded from the pristine sample is very complex and significantly different to the S 2p spectrum recorded from the sample after its treatment with KOH. It was necessary to deconvolute the S 2p spectrum of the pristine sample into five S $2p_{3/2}$ component peaks (*V*, *W*, *X*, *Y*, and *Z* drawn in black, the corresponding S $2p_{1/2}$ peaks were drawn in grey). After the sample's treatment with KOH, two binding states of sulfur seemed to be disappeared. The two S 2p spectra in Figure 5 (right column) clearly show a component peak *V* (and its corresponding *V'* component peak) resulting from the sulfide-like bonded sulfur atoms in the PEDOT molecules. A second component peak *Y* arose from the sulfur atoms of the PSS ($R\text{–}\underline{S}O_3^-$). In acid environment H_3O^+ ions coming from the dissociation of PSS ($R\text{–}\underline{S}O_3H + H_2O \rightleftharpoons R\text{–}\underline{S}O_3^- + H_3O^+$) are able to protonate the PEDOT molecules, where polarons and bipolarons can be formed (Figure 6). The positive charges, which are delocalized over the π-electron systems of the PEDOT molecules, shift the binding energy of the sulfide-like bonded sulfur to higher values (additional attractive Coulomb interaction between the positive charge and the negative charge of the photoelectron escaped during the sample's interaction with X-rays). Hence, component peaks *W* and *X* appear from polarons and bipolarons. The sample's treatment with KOH strongly reduces the number of H_3O^+ ions by their neutralization ($H_3O^{+}+OH^- \rightleftharpoons 2\,H_2O$). As a result, the degree of protonation of the PEDOT was significantly reduced. In the S 2p spectrum of the KOH treated sample component peak *X* (showing the bipolarons) was completely disappeared. However, the presence of component peak *W* makes sure that also in strong basic environment some of the PEDOT molecules are protonated and able to transport charges. Protonated PEDOT molecules (present in acidic environment as polarons and bipolarons) are able to form salt pairs ($R\text{–}SO_3^{-}\cdots{}^{+}[PEDOT]$, water molecules can be included in the electrostatic bond via hydrogen bonds) with the dissociated PSS species. The decreased electron density on the $R\text{–}SO_3^-$ species involved in such aggregates shifts the binding energy of sulfur to slightly higher values. The corresponding component peak *Z* was found at 169 eV. Photoelectrons from sulfur of non-dissociated PSS species ($R\text{–}SO_3H$), which is only present in strong acidic environment, also contributed to component peak *Z*. Furthermore, the intensity of the S 2p peak at 169 eV corresponded to the $R\text{–}SO_3^-$ group is significantly reduced for the KOH-treated sample relative to the pristine sample and this may be explained by dissociation of a part of PSS component from PEDOT:PSS complex occurring upon addition of base. Indeed, because PEDOT is a more hydrophobic component than PSS, it should have a lower surface energy than PSS and therefore PEDOT should be preferentially segregated above the dissociated part of PSS. On the other hand, XPS reveals the composition of the very topmost layer (<10 nm) and should reflect this vertical segregation.

Absorption spectra

As discussed above, addition of KOH into the PEDOT:PSS dispersions deprotonates PEDOT chains which, in turn, decreases amount of bipolaron-like species. This agrees with transformations of UV-vis-near-IR spectra and the color change from a bright blue inherent to acidic, highly doped state of PEDOT:PSS to a dark blue or purple color characteristic to its deprotonated (and/or dedoped) form. Particularly, for the p-conducting PEDOT:PSS the majority charge carriers are positively charged polarons and bipolarons, which show distinct absorption in the near infrared region. The optical UV-Vis-NIR spectra were taken between 400 nm and 2,400 nm on spin coated PEDOT:PSS thin films and are shown in Figure 7.

The unmodified PEDOT:PSS shows a strong absorption band at 1,300 nm–2,400 nm which is attributed to bipolarons (Park et al. 2013; Massonnet et al. 2014). The polaron absorption between 700 nm–1,300 nm and the absorption of the neutral polymer chain between 400 nm–700 nm is marginal for the untreated PEDOT:PSS. With increasing content of KOH the bipolaron absorption decreases while the absorption of polarons and the neutral polymer chain increases. However, the polaron absorption decreases again for a concentration of 240 mM while showing distinct neutral polymer chain absorption. As a result, it can be shown that addition of KOH changes the PEDOT state from bipolarons to polarons and up to neutral chains.

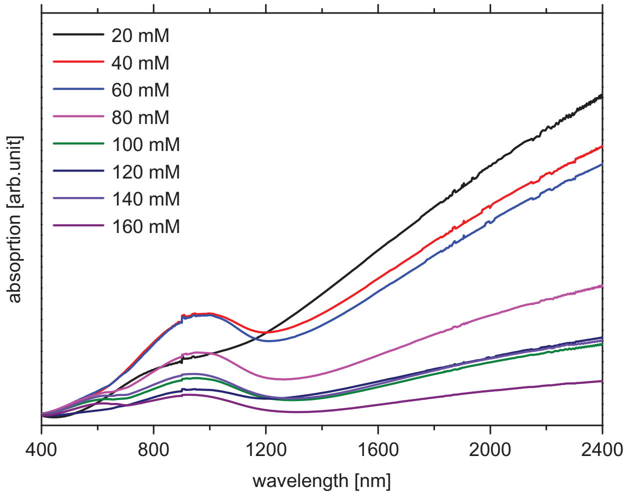

Figure 7: UV-Vis-NIR spectra of PEDOT:PSS PH1000 (normalized to layer thickness) in the presence of KOH at different concentrations. The small bump at 900 nm is due to detector change in Cary 5000 instrument.

Thermoelectric properties

The results of the thermoelectric characterization are shown in Figure 8.

Unmodified PEDOT:PSS shows here an electrical conductivity of 220 S/m. With increasing amount of added KOH up to 70 mM the electrical conductivity firstly decreases to ~50 S/m. As the electrical conductivity is proportional to charge carrier mobility μ and the charge carrier density n according to the formula $\sigma = en\mu$, the observed decrease in conductivity is consistent with decreased concentration of charge carriers – polarons and bipolarons.

Interestingly, further increase of amount of added KOH leads to a local enhancement of conductivity up to 150 S/m observed at 110 mM; however, further increase of the base content again decreases the conductivity to 50 S/m. Although exact reason for such a non-monotonic dependence is not clear at the moment, it can be attributed to complex rearrangements occurring upon addition of base.

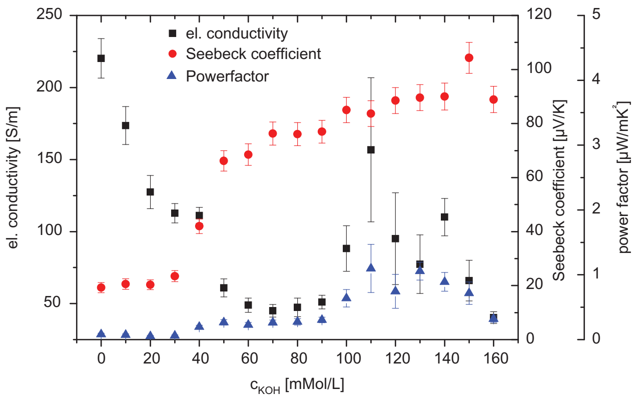

Figure 8: Electrical conductivity, Seebeck coefficient and power factor of PEDOT:PSS PH1000 with variation of KOH concentration.

Because the Seebeck coefficient α is conversely proportional dependent on the charge carrier density $\alpha \propto \frac{1}{n}$ (Stöcker, Köhler, and Moos 2012), it should increase with the decrease of carrier concentration. This assumption is in a full agreement with experimental data. Thus, the Seebeck coefficient of untreated PEDOT:PSS (highly doped PEDOT with high charge carrier density) is in the range of 15 µV/K. Increasing of the KOH content leads to a reduction of charge carriers and an increase in the Seebeck coefficient. The most step increase of the Seebeck coefficient (from 20 µV/K to 65 µV/K) is observed between KOH concentrations of 30 mM to 50 mM. At higher concentrations of base the Seebeck coefficient increases to a maximum in the range of 90 µV/K. We can observe a similar trend when comparing the Seebeck coefficient and pH value vs. KOH concentration (compare Figure 2 and Figure 8). The Seebeck coefficient vs. pH value is shown in Figure 9.

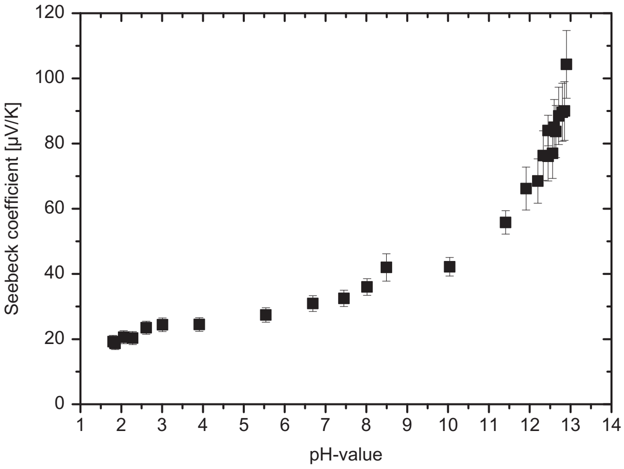

Figure 9: Seebeck coefficient of PEDOT:PSS thin films in dependence of the pH value of its associated dispersion.

It can be seen that the Seebeck coefficient increases almost linearly with increasing pH value in the range of pH from 2 to 12. At a pH of ~ 12 (corresponding to a KOH concentration of 50 mM) the Seebeck coefficient increases more steeply (i.e., the slope increases from factor of 4 to factor of 40). In this concentration range also the polaron absorption starts to increase significantly. This indicates that at a given pH of 12 the alkaline conditions affect directly the protonated PEDOT chain causing deprotonation/dedoping. From this point, only a slight change in the pH value increases the Seebeck coefficient dramatically. However, it should be noted that at very acidic pH values significantly larger amounts of KOH are required in order to change the pH value than near the equivalence point.

The calculated thermoelectric power factor for the unmodified PEDOT:PSS film is 0.08 µW/mK². Increasing the KOH concentration also increases the power factor by one order of magnitude to a maximum of approx. 1.1 µW/mK² at concentrations between 110130 mM KOH. Above-presented results show that PEDOT:PSS can be modified by means of a wet chemical alteration before deposition/printing. In the following PEDOT:PSS printing paste will be investigated for a dispenser printing process.

Dedoping of PEDOT:PSS SV3

For printing a polymer TEG the PEDOT:PSS SV3 paste was used. The printing paste was modified by using KOH with concentrations varied between 0 mM and 150 mM. The thermoelectrical properties are shown in Figure 10.

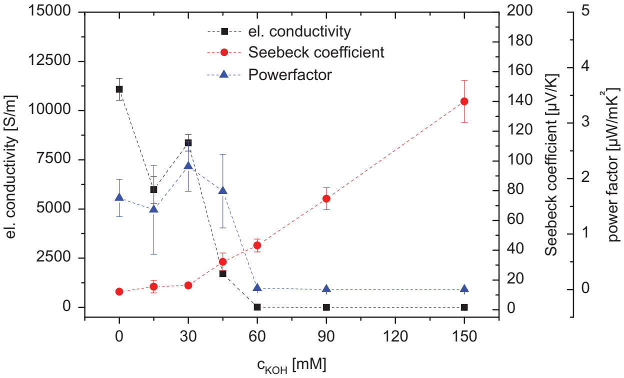

Figure 10: Electrical conductivity, Seebeck coefficient and power factor of PEDOT:PSS SV3 with variation of KOH concentration. The lines are meant to guide the eye.

In general PEDOT:PSS SV3 shows the same behavior as PEDOT:PSS PH1000 when treated with KOH. However, it is difficult to compare absolute values due to different compositions and doping level of tested PEDOT:PSS composites as well as sample preparation procedures (preparation of thick films for PEDOT:PSS SV3 films are much thicker than PEDOT:PSS PH1000 films). By adding KOH the electrical conductivity decreases from 11,000 S/m to 0.02 S/m whereas the Seebeck coefficient increases from 12 µV/K up to 140 µV/K for untreated versus treated with the highest base concentration, respectively. The power factor has its maximum of 2.2 µW/mK² at around 30 mM of KOH.

Subsequently, a flexible PEDOT:PSS unileg TEG will be printed by using reduced PEDOT:PSS SV3 printing paste in order to generate a maximum power.

Printing of a thermoelectrical generator

Unileg-TEG strips, 253 mm in length, having 61 unicouples, were printed by using base-modified (with 30 mM KOH) PEDOT:PSS SV3 printing paste and silver by means of dispenser printer. Printed line widths for the PEDOT:PSS and silver is ~ 1 mm. The leg length of each unicouple is 18 mm. As a result, the TEG strips are fully bendable (see Figure 11). Such strips could be either implemented as rigid TEGs coiled up like scotch tape. Such a design have the advantage of showing a high number of thermocouples per area resulting in high output voltages per area. Additionally, a vertical TEG design allows these strips to be cut easily into desired form/contour in order to match non planar heat sources.

The TEG strips were coiled up onto an aluminum adapter and characterized. The internal electrical resistance is ~7.7 kΩ. The TEG was exposed to a temperature gradient between 10 and 90 K with a matched load.

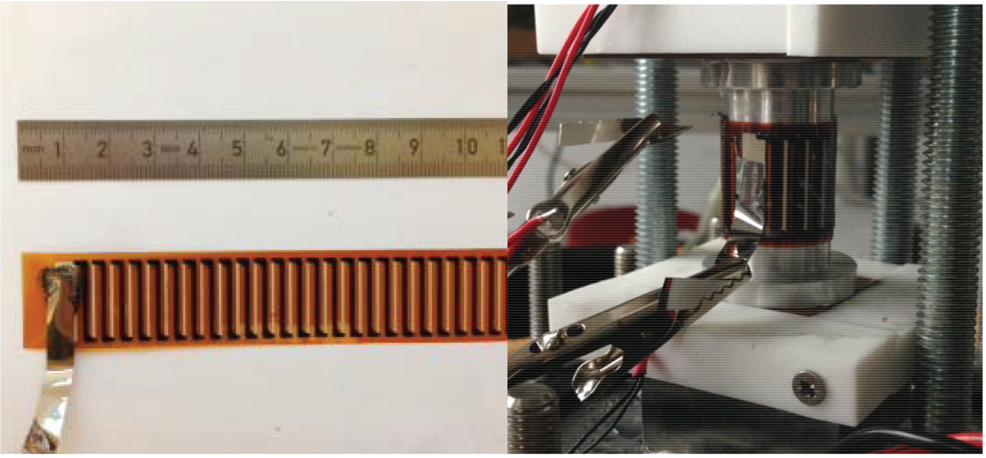

Figure 11: Dispenser printed fully flexible polymer unileg-TEG (left). Electrical characterization setup of a polymer-TEG-strip mounted on an aluminum adapter (right).

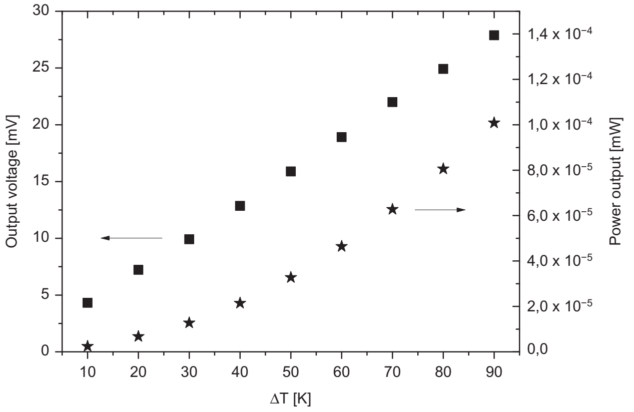

Figure 12: Output voltage and power output for printed flexible polymer-TEG under matched load.

The output voltage and power output is presented in Figure 12. It is shown that increase of the temperature gradient also increases the output voltage. At a given ΔT of 30 K, the output voltage is ~ 10 mV and it increases linearly to ~25 mV at ΔT of 90 K. Admittedly, this low output voltage results in an low power output of ~ 100 nW (at $\Delta T = 90$ K) due to the high internal resistance of the generator of approx. 7 kΩ.

This discloses a major challenge for polymeric-TEGs. The electric conductivity as well as the electrical contact resistances between the metallic and polymer material show the highest contributions to the internal resistance of a polymer-TEG. If we overcome the mismatch in energy level between the metal and the polymer to an overall internal resistance of ~100 Ω, the power output would increase by a factor of ~100. However, the use of printing techniques like dispenser printer shows an appealing approach in the fabrication of flexible polymer-TEGs.

Conclusion

In this work, we have successfully shown the modification of PEDOT:PSS PH1000 and SV3 with KOH before film formation. The thermoelectric properties were investigated by Seebeck coefficient and electrical conductivity measurements as well as UV-Vis-NIR spectroscopy. It could be shown that the Seebeck coefficient can be adjusted by changing the pH value of PEDOT:PSS dispersions (see Figures 8 and 10). It is assumed that the change of the pH value to alkaline conditions leads to deprotonation of PEDOT chains which is equivalent to their dedoping, which could be observed in UV-Vis-NIR spectroscopy. XPS measurements confirm dedoping of PEDOT chains occurring upon addition of KOH. Furthermore, they show reduction of intensity as well as narrowing of S 2p signal of RS$\underline{O}_3^-$ group which may be explained by dissociation of a part of PSS component from PEDOT:PSS complex occurring upon addition of base leading to enrichment of the topmost layer with the PEDOT component. Due to the KOH treatment, the Seebeck coefficient and electrical conductivity varying between 15 μV/K and 90 μV/K and 11 kS/m and 0.02 S/m, respectively. The modified material was subsequently dispenser-printed into a fully flexible polymer unileg-TEG strips with 61 unicouples. The printed unileg-TEG shows high internal resistance of approx. 7 kΩ resulting in a low power output of ~ 100 nW (at 90 K). However, the results presented here are promising in terms of easy and up scalable processing for flexible TEG manufacturing. Challenges like the electrical contact resistance of polymer-metal interfaces, as well as the polymer material properties itself has to be improved though.

Acknowledgements: This work has received partial funding from the European Unions Seventh Framework Programme for research, technological development and demonstration under the grant agreement No 604647. The authors would also like to thank Beate Leupold and Susann Schulz from Fraunhofer IWS Dresden for UV-Vis-NIR measurements.

Funding: European Union's Seventh Framework Programme 604647.

References

Ahonen, H. J., J. Lukkari, and J. Kankare. 2000. N- and p-Doped Poly (3,4-Ethylenedioxythiophene): Two Electronically Conducting States of the Polymer. *Macromolecules* 33:678793.

Beamson, G., and D. Briggs. 1992. *High Resolution XPS of Organic Polymers, the Scienta ESCA300 Database*. Chichester: Wiley.

Bubnova, O., Z. U. Khan, A. Malti, S. Braun, M. Fahlman, M. Berggren, and X. Crispin. 2011. Optimization of the Thermoelectric Figure of Merit in the Conducting Polymer Poly (3,4-Ethylendioxythiopene). *Nature Materials*. DOI:10.1038/NMAT3012.

Chen, A., D. Madan, P. K. Wright, and J. W. Evans. 2011. Dispenser-Printed Planar Thick-Film Thermoelectric Energy Generators. *Journal of Micromechanics and Microengineering* 21 (10). DOI:10.1088/09601317/21/10/104006.

Dani, I., A. Roch, L. Stepien, C. Leyens, M. Greifzu, and M. von Lukowicz. 2013. Energy Turnaround: Printing of Thermoelectric Generators. In *Digital Product and Process Development Systems*, edited by G. L. Kovacs. 1st ed. Berlin: Springer.

Elschner, A., S. Kirchmeyer, W. Lovenich, U. Merker, and K. Reuter. 2010. *PEDOT: Principles and Applications of an Intrinsically Conductive Polymer*. Taylor Francis Group: CRC Press.

Jönnson, S. K. M., J. Birgerson, X. Crispin, G. Greczynski, W. Osikowicz, A. W. Denier, W. R. van der Gon, and S. M. Fahlman. 2003. The Effects of Solvents on the Morphology and Sheet Resistance in Poly(3,4-Ethylenedioxythiophene) Polystyrenesulfonic Acid (PEDOTPSS) Films. *Synthetic Metals* 139:110.

Kim, J. Y., J. H. Jung, D. E. Lee, and J. Joo. 2002. Enhancement of Electrical Conductivity of Poly(3,4-Ethylenedioxythiophene)/Poly(4-Styrenesulfonate) by a Change of Solvents. *Synthetic Metals* 126:31116.

Kim, T. Y., C. M. Park, J. E. Kim, and K. S. Suh. 2005. Electronic, Chemical and Structural Change Induced by Organic Solvents in Tosylate-Doped Poly(3,4-Ethylenedioxythiophene) (PEDOT-OTs). *Synthetic Metals* 149 (23):16974.

Kim, G.-H., L. Shao, K. Zhang, and K. P. Pipe. 2013. Engineered Doping of Organic Semiconductors for Enhanced Thermoelectric Efficiency. *Nature Materials*. DOI:10.1038/NMAT3635.

de Kok, M. M., M. Büchel, P. van der Weijer, E. A. Meulenkamp, S. H. P. M. de Winter, A. J. G. Mank, H. J. M. Vorstenbosch, C. H. L. Weijtens, and V. van Elsbergen. 2004. Modification of PEDOT: PSS as Hole Injection Layer in Polymer LEDs. *Physica Status Solidi (A)* 201 (6):134259.

Lock, J. P., J. L. Lutkenhaus, N. S. Zacharia, S. G. Im, P. T. Hammond, and K. K. Gleason. 2007. Electrochemical Investigation of PEDOT Films Deposited via CVD for Electrochromic Applications. *Synthetic Metals* 157:8948.

MacDiarmid, A. G., and A. J. Epstein. 1994. The Concept of Secondary Doping as Applied to Polyaniline. *Synthetic Metals* 65(23):10316.

Massonnet, N., A. Carella, O. Jaudouin, P. Rannou, G. Laval, C. Cellea, and J.-P. Simonato. 2014. Improvement of the Seebeck Coefficient of PEDOT:PSS by Chemical Reduction Combined with a Novel Method for Its Transfer Using Free-Standing Thin Films. *Journal of Materials Chemistry C*. DOI: 10.1039/c3tc31674b.

Masubuchi, S., S. Kazama, K. Mizoguchi, M. Honda, K. Kume, R. Matsushita, and M. Matsuyama. 1993. Metallic Transport Properties in Electrochemically as-Grown and Heavily Doped Polythiopene and Poly(3-Methylthiopene). *Synthetic Metals* 57 (2):49627.

Mateeva, N., H. Niculescu, J. Schlenoff, and L. R. Testardi. 1998. Correlation of Seebeck Coefficient and Electric Conductivity in Polyaniline and Polypyrrole. *Journal of Applied Physics* 83 (6):311117.

Meen, T.-H., K.-L. Chen, Y.-H. Chen, W.-R. Chen, D.-W. Chou, W.-H. Lan, and C.-J. Huang. 2013. The Effects of Dilute Sulfuric Acid on Sheet Resistance and Transmittance in Poly(3,4-Ethylenedioxythiophene):Poly(Styrenesulfonate) Films. *International Journal of Photoenergy*. http://dx.doi.org/10.1155/2013/843410.

Moulder, J. F., W. F. Stickle, P. E. Sobol, and K. D. Bomben. 1992. *Handbook of X-Ray Photoelectron Spectroscopy*. Edited by J. Castian and R.C. King Jr. Eden Prairie: Perkin-Elmer Corp.

Oeter, U., C. Ziegler, and W. Göpel. 1993. Undoped and Doped Oligothiophenes: An in-Sity XPS-, UPS-, and HREELS-Study. *Berichte Der Bunsengesellschaft Für Physikalische Chemie* 17:44851.

Osterholm, J.-E., P. Passiniemi, H. Isotalo, and H. Stubb. 1987. Synthesis and Properties of $FeCl_3$-Doped Polythiopene. *Synthetic Metals* 18 (13):21318.

Ouyang, J. 2013. Solution-Processed PEDOT:PSS Films with Conductivities as Indium Tin Oxide Through a Treatment with Mild and Weak Organic Acids. *ACS Applied Material Interfaces* 5 (24):130828.

Ouyang, J., Q. Xua, C.-W. Chua, Y. Yanga, G. Lib, and J. Shinar. 2004. On the Mechanism of Conductivity Enhancement in Poly(3,4-Ethylenedioxythiophene):Poly(Styrene Sulfonate) Film Through Solvent Treatment. *Polymer* 45:844350.

Park, Y. W. 1991. Structure and Morphology: Relation to the Thermo Properties of Conductive Polymers. *Synthetic Metals* 45 (2):17382.

Park, T., C. Park, B. Kim, H. Shin, and E. Kim. 2013. Flexible PEDOT Electrodes with Large Thermoelectric Power Factors to Generate Electricity by the Touch of Fingertips. *Energy and Environmental Science* 6:78892.

Russat, J. 1988. Characterization of Polyamic Acid/Polyimide Films in the Nanometric Thickness Range from Spin-Deposited Polyamic Acid. *Surface and Interface Analysis* 8 (11):41420.

Snyder, G. J., and E. S. Toberer. 2008. Complex Thermoelectric Materials. *Nature Materials* 7:10514.

Stöcker, T., A. Köhler, and R. Moos. 2012. Why Does the Electrical Conductivity in PEDOT:PSS Decrease with PSS Content? A Study Combining Thermoelectric Measurements with Impedance Spectroscopy. *Journal of Polymer Science (B) Polymer Physics* 50:97683.

Sun, Y., P. Sheng, C. Di, F. Jiao, W. Xu, D. Qiu, and D. Zhu. 2012. Organic Thermoelectric Materials and Devices Based on p- and n-Type Poly(Metal 1,1,2,2-Ethenetetrathiolate)s. *Advanced Materials* 24:9327.

Weijtens, C., V van Elsbergen, M. de Kok, S. de Winter. 2005. Effect of the alkali metal content on the electric properties of PEDOT: PSS. *Organic Electronics* 6 (2):97–104 doI: 10.1016/j.orgel.2005.02.005.

Yan, H., N. Sada, and N. Toschima. 2002. Thermal Transporting Properties of Electrically Conductive Polyaniline Films as Organic Thermoelectric Materials. *Journal of Thermal Analysis and Calorimetry* 69 (3):8817.

Zuzok, R., A. B. Kaiser, W. Pukacki, and S. Roth. 1991. Thermoelectric Power and Conductivity of Iodine-Doped New Polyacetylene. *The Journal of Chemical Physics* 95 (2):12705.